SUITABLE CONTROL LAWS TO PATH TRACKING IN OMNIDIRECTIONAL WHEELED MOBILE ROBOTS SUPPORTED BY THE MEASURING OF THE ROLLING PERFORMANCE

C. A. Peña Fernández* J. J. F. Cerqueira* A. M. N. Lima†

*Laboratório de Robótica - Programa de Pós-graduação em Engenharia Elétrica
da Escola Politécnica da Universidade Federal da Bahia
Rua Aristides Novis, 02, Federação, 40210-630, Salvador, Bahia, Brasil
Telefone:+55-71-3203-9760.

†Departamento de Engenharia Elétrica do Centro de Engenharia Elétrica e Informática da
Universidade Federal de Campina Grande
Rua Aprigio Veloso, 882, Universitário, 58429-970, Campina Grande, Paraíba, Brasil
Telefone:+55-83-2101-1000.

Email: cesar.pena@ufba.br,jes@ufba.br,amnlima@dee.ufcg.edu.br

Abstract— This work proposes a method in order to choose suitable control laws supported in the measuring of the rolling performance in omnidirectional wheeled mobile robots when the holonomic kinematic constraints are not fully satisfied. One important reason that causes such dissatisfaction is the slip presents at wheels and, consequently, the inappropriate conditions for the rolling. The appropriate rolling conditions for omnidirectional wheeled mobile robots are defined by zero slip rate (i.e., $\dot{s} = 0$) and nonzero slip (i.e., $s \neq 0$) (Fernández et al., 2012). By using the singular perturbation theory the slip can be included into overall dynamic of the mobile robot and it is possible to project control actions that mitigate the slip. Here, an expression to measuring the slip rate is derived in order to accessing the rolling performance in the mobile robot. Supporting us in such expression is possible to choose the suitable control law that ensures fully the appropriate rolling conditions. This methodology was applied in an experimental platform called AxeBot that is being constructed in the Robotics Laboratory at University Federal of Bahia and that uses odometry for the self-localization.

Keywords— Omnidirectional mobile base, slip, corrective control actions, rolling performance, singular perturbation theory.

Resumo— Este trabalho propõe um método para escolher leis controle apropriadas apoiado na medida do desempenho do rolamento em robôs móveis omnidirecionais quando as restrições cinemáticas holonômicas não são completamente satisfeitas. Uma das razões mais importantes que causa tal insatisfação é o escorregamento presente nas rodas e, consequentemente, as condições inapropriadas de rolamento. As condições apropriadas de rolamento para robôs móveis omnidirecionais são definidas por uma variação de escorregamento nula e por um valor de escorregamento diferente de zero (Fernández et al., 2012). Pelo uso da teoria de perturbações singulares o escorregamento pode ser incluído na dinâmica geral do robô e é possível projetar leis de controle que atenuam o escorregamento. Aqui, uma expressão para medir a variação do escorregamento é derivada a fim de acessar o desempenho do rolamento no robô móvel. Apoiando-nos em tal expressão é possível escolher a lei de controle adequada que garante a satisfação das condições de rolamento apropriada. Esta metodologia foi aplicada em uma plataforma experimental chamada Axebot que está sendo construída no Laboratório de Robótica da Universidade Federal da Bahia e que usa odometria para sua auto-localização.

Palavras-chave— Base móvel omnidirecional, escorregamento, ações de controle corretivas, desempenho do rolamento, teoria de pertubações singulares.

1 Introduction

In this paper we have formulated a methodology to choose the suitable control laws such that the appropriate rolling conditions are satisfied (Fernández et al., 2012). We apply our methodology to validate a control law with corrective actions for the trajectory tracking problems in the AxeBot, an omnidirectional wheeled mobile robot (OWMR) that is being constructed in the Robotics Laboratory at University Federal of Bahia for research and development of the trajectory control (see Fig. 1(a)). To implement this methodology is considered that omnidirectional motion of the Axebot do not satisfy its holonomic kinematic constraints as a consequence of the slippage. A condition usually considered for trajectory tracking problems in mobile robots is the ideal rolling assumption, i.e., the wheels of a mobile robot are assumed to roll without slipping. But disregarding the slip of wheels in the dynamic model leads us to path tracking problems (Fernández and Cerqueira, 2009a; Motte and Campion, 2000). When the robot is either accelerating, or decelerating, or cornering at a high speed the wheel slip becomes an issue and the ideal rolling assumption is not satisfied (Fernández and Cerqueira, 2009b; Fernández and Cerqueira, 2009a). If the slip is not taken into account, a designed task may not be completed and a stable system may even become unstable. One of the most important reasons for this problem is when the trajectory tracking is made by using odometry to calculating the cartesian position. This methodology has been widely used, largely because of its easy implementation, but its disadvantage is the unlimited accumulation of errors in the control scheme due to slip in the wheels, among other intrinsic properties of the surface motion (Song and Wang, 2009; Ivankjo et al., 2004; Bahari et al., 2008; Trojnacki, 2013). In the AxeBot, the self-

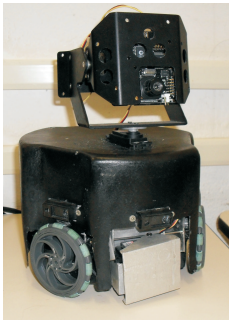

(a)

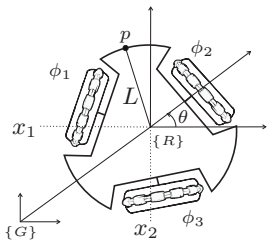

(b)

Figura 1: Photograph of (a) the experimental platform AxeBot and (b) Kinematic structure of the omnidirectional wheeled mobile robot with global frame $\{G\}$ and local frame $\{R\}$.

localization is made with Odometry, thus this platform offers a convenient problem situation which will allow to verify if the control law applied will guarantee a good rolling performance.

With the problem of the slipping we have considered that the AxeBot can be modeled by a singularly perturbed model. Assuming that there exists an invariant manifold for the slip, corrective control actions are projected by using the singular perturbation theory such that slip in the wheels is mitigated (Motte and Campion, 2000; D'andréa-novel et al., 1995). We propose to use an expression to caracterize the slip rate related to trajectory tracking problems as tool to measuring the rolling performance. By using the experimental platform AxeBot such tool is used as support to choose the suitable control law.

This paper is organized as follows: In Section 2, the key aspects regarding OWMRs and the inclusion of slip nonlinearity into the proposal of the singularly perturbed model are discussed. In Section 3 is shown the proposal to measuring the rolling performance. In Section 4 an invariant manifold for slip is defined and computed such that corrective control actions can be projected to minimize the errors into the control scheme due to the existence of slip. In Section 5 the proposed approach is used for accessing the achievable closed-loop performance with the corrective control actions projected and it is discussed the observations obtained. Finally, conclusions and closing remarks are shown in Section 6.

2 Mathematical Dynamic Model

The configuration of AxeBot mobile robot can be fully described by the vector $q \in \mathbb{R}^6$ of generalized coordinates defined by

$$q = [x_1 \; x_2 \; \theta \; \phi_1 \; \phi_2 \; \phi_3]^T$$

where $\{x_1, x_2, \theta\}$ is the set of coordinates associated with the cartesian position of the local frame $\{R\}$ into the global frame $\{G\}$ and guidance of mobile base, and $\{\phi_1, \phi_2, \phi_3\}$ is the set associated with the angular position of each wheel [which can not be controlled independently] (see Fig. 1(b)).

The kinematic constraints can be expressed as the Pfaffian constraint (Motte and Campion, 2000)

$$A^T(q)\dot{q} = 0 \tag{1}$$

where $A(q)$ is the matrix with the holonomic kinematic constraints defined by

$$A(q) = \begin{bmatrix} -\sin\alpha & \sin\theta & \sin\beta \\ -\cos\alpha & -\cos\theta & -\cos\beta \\ b & b & b \\ r & 0 & 0 \\ 0 & r & 0 \\ 0 & 0 & r \end{bmatrix} \triangleq \left[\begin{array}{c} A_1(\theta) \\ \hline A_2(\theta) \end{array}\right],$$

where $\alpha = \theta - \frac{2\pi}{3}$, $\beta = \theta + \frac{2\pi}{3}$, b is the displacement from each of driving wheels to the axis of symmetry of mobile base, r is the radius of each wheel.

Provided that the ideal kinematic constraints are not satisfied [i.e., $A^T(q)\dot{q} \neq 0$], then the generalized velocity vector $\dot{q}$ may be written as

$$\dot{q} = S(q)v + A(q)\varepsilon s, \tag{2}$$

such that

$$A^T(\theta)S(q) = 0, \tag{3}$$

where

$$S(q) = \begin{bmatrix} \cos\theta & \sin\theta & 0 \\ -\sin\theta & \cos\theta & 0 \\ 0 & 0 & 1 \\ -\sqrt{3}/2r & 1/2r & b/r \\ 0 & -1/r & b/r \\ \sqrt{3}/2r & 1/2r & b/r \end{bmatrix} \triangleq \left[\begin{array}{c} S_1(\theta) \\ \hline S_2(\theta) \end{array}\right],$$

is the Jacobian, $v = [v_1 \; v_2 \; v_3]^T$ is the vector that contains the velocities at the wheels and $s = [s_1 \; s_2 \; s_3]^T$ contains the slip at each wheel. This last one can be considered as instrumental vector in sense of accessing the violations of the ideal kinematic constraints in OWMRs. It is important to mention that when there is slip, the vector q becomes an apparent quantity $\tilde{q}$.

As usual, the dynamic model for such mobile base is given by

$$M\ddot{q} = \Lambda + Bu_\varepsilon + A(\theta)\lambda \tag{4}$$

where $M = \text{diag}\,(M \; M \; I_c \; I_w \; I_w \; I_w)$, $\Lambda = 0_{6\times 1}$, $B = \begin{bmatrix} 0_{3\times 3} \\ I_{3\times 3} \end{bmatrix}$ are the inertia matrix, the centripetal and coriolis torques [equal to zero because is assumed that the geometrical center coincides with the mass center] and a full rank matrix, respectively. The parameter M is the mass of mobile base, I_c is the moment of inertia of mobile base about a vertical axis through the intersection of the axis of symmetry with the driving wheel axis and I_w is the moment of inertia of each driving wheel about the wheel axis. The vector u_ε represents of the input forces or torques provided by the actuators and $\lambda \in \mathbb{R}^3$ represents of Lagrange multipliers (Balakrishna and Ghosal, 1995).

2.1 Singularly perturbed model

The singularly perturbed formulation to the dynamic of AxeBot is defined by the following state-space description:

$$\dot{x} = B_0(q)v + [\varepsilon B_1(q) + B_2(q)]\, s + B_3(q)u_\varepsilon \tag{5}$$

$$\varepsilon\dot{s} = C_0(q)v + [\varepsilon\, C_1(q) + C_2(q)]\, s + C_3(q)u_\varepsilon \tag{6}$$

$$y = P_0(q) \tag{7}$$

where $x = \left[q^T \; v^T\right]^T$ can be used to denote the "slow" variables and s beyond its instrumental meaning can be used to denote the "fast" variables; ε is a small positive parameter, $u_\varepsilon = [u_{\varepsilon,1} \; u_{\varepsilon,2} \; u_{\varepsilon,3}]^T$ are the manipulated inputs associated with the torques at the motors and $y = [y_1 \; y_2]^T$ are the cartesian coordinates

of a point p located at a distance L of the symmetry axle of the robot, i.e.:

$$y = P_0(q) \triangleq \begin{bmatrix} x_1 - L\sin\theta \\ x_2 + L\cos\theta \end{bmatrix} = P_0(\theta). \tag{8}$$

The above matrices $B_i(q)$, $C_i(q)$, for $i = 0, 1, 2, 3$, are successively:

$$B_0(q) = \begin{bmatrix} S(\theta) \\ a_1 \ a_2 \ a_3 \\ a_4 \ a_5 \ a_6 \\ a_7 \ a_8 \ a_9 \end{bmatrix}, \quad B_1(q) = \begin{bmatrix} A(\theta) \\ a_{10} \ a_{11} \ a_{12} \\ a_{13} \ a_{14} \ a_{15} \\ a_{16} \ a_{17} \ a_{18} \end{bmatrix},$$

$$B_2(q) = \begin{bmatrix} 0_{6\times 3} \\ a_{28} \ a_{29} \ a_{30} \\ a_{31} \ a_{32} \ a_{33} \\ a_{34} \ a_{35} \ a_{36} \end{bmatrix}, \quad B_3(q) = \begin{bmatrix} 0_{6\times 3} \\ a_{19} \ a_{20} \ a_{21} \\ a_{22} \ a_{23} \ a_{24} \\ a_{25} \ a_{26} \ a_{27} \end{bmatrix},$$

$$C_0(q) = \begin{bmatrix} a_{37} \ a_{38} \ a_{39} \\ a_{40} \ a_{41} \ a_{42} \\ a_{43} \ a_{44} \ a_{45} \end{bmatrix}, \quad C_1(q) = \begin{bmatrix} a_{46} \ a_{47} \ a_{48} \\ a_{49} \ a_{50} \ a_{51} \\ a_{52} \ a_{53} \ a_{54} \end{bmatrix},$$

$$C_2(q) = \begin{bmatrix} a_{64} \ a_{65} \ a_{66} \\ a_{67} \ a_{68} \ a_{69} \\ a_{70} \ a_{71} \ a_{72} \end{bmatrix}, \quad C_3(q) = \begin{bmatrix} a_{55} \ a_{56} \ a_{57} \\ a_{58} \ a_{59} \ a_{60} \\ a_{61} \ a_{62} \ a_{63} \end{bmatrix},$$

being a_i, for $i = 1, \ldots, 72$, known values and defined by

$$a_i \triangleq a_i(v_\eta, \delta, D_o, G_o),$$

where the parameter v_η is the velocity of the wheel center and δ is a "small" positive constant to avoid the numerical problem for small values of v_η [i.e., for small values of v_η, it is replaced by $v_\eta + \delta$]. The parameters D_o and G_o are normalized values defined by

$$D_o = \varepsilon D \qquad \text{and} \qquad G_o = \varepsilon G,$$

where D and G are the stiffness coefficients for the transversal and longitudinal movements of each wheel, respectively.

Assumption 1 *The longitudinal and transversal stiffness coefficients (G and D, respectively) are the same for the three wheels and*

$$\varepsilon = \inf\{1/G, 1/D\}.$$

Assumption 2 *The velocities of the three driving wheels at their center are taken to be identical, and more precisely, equal to their average:*

$$v_\eta = \left(\dot{x}_1^2 + \dot{x}_2^2 + \dot{\theta}^2\right)^{1/2}. \tag{9}$$

2.2 Interaction forces at wheels

Since OWMRs have only constraints associated with *rolling* conditions, in this work, the contact forces are represented in terms of the relationship between the longitudinal slip ratio of each wheel, s_i, and its respective friction coefficient μ_i.

Assumption 3 *The friction coefficients μ_i (for $i = 1, 2, 3$) are taken to be identical due to symmetric mass distribution, and more precisely, equal to*

$$\mu_i = M_r \frac{3}{Mg} \dot{v}_i \triangleq z_o \dot{v}_i$$

where M_r is the mass of each driving wheel and g is the gravity.

Burckhardt's model, for instance, can be used to describe the nonlinear characteristics of the contact forces (Fernández et al., 2012; Canudas de Wit et al., 2003). For our purpose, this map is defined by

$$\mu_i = c_1\left(1 - e^{-c_2 s_i}\right) - c_3 s_i\Big|_{c_1=1;\, c_2=2;\, c_3=0.1}, \tag{10}$$

for $i = 1, 2, 3$. Where the parameters c_1, c_2, c_3 are setting for humidity conditions, as shown in (Canudas de Wit et al., 2003). In this mapping $s_i \in [-1, +1]$ and $\mu_i \in \mathbb{R}$.

3 Rolling dynamic analysis

The appropriate rolling conditions in the OWMR motion can be defined by

$$\begin{cases} s \neq 0 \\ \dot{s} = 0. \end{cases} \tag{11}$$

The condition $s \neq 0$ means that the mechanical torques are not large enough to ensure that the wheel-surface contact point stay stationary. It is important to point out that such condition is an inherent and proper feature of OWMRs motion (Fernández et al., 2012; Balakrishna and Ghosal, 1995).

3.1 Proposal to measuring the rolling performance

The rolling dynamics are analyzed according to the satisfaction of the appropriate rolling condition defined in (11). In following will be presented an analysis associated with the longitudinal rolling that will allow to define a criteria to choose a suitable control law.

The apparent linear velocities of wheels can be associated with the apparent linear velocity of the mobile base by using (2) and via the pseudo-inverse matrix $S^+(q)$

$$\begin{aligned} v &= S^+(q)\left(\dot{q} - A(q)\varepsilon s\right) \\ &\triangleq S^+(\theta)\begin{bmatrix} \dot{x}_1 - A_1(\theta)\varepsilon s & \ldots & \dot{\phi}_3 - A_6(\theta)\varepsilon s \end{bmatrix}^T \\ &\triangleq S^+(\theta)\underbrace{\begin{bmatrix} \dot{\tilde{x}}_1 & \dot{\tilde{x}}_2 & \dot{\tilde{\theta}} & \ldots & \dot{\tilde{\phi}}_3 \end{bmatrix}^T}_{\dot{\tilde{q}}} \end{aligned}$$

where $A_i(\theta)$ represent the i-th row of $A(\theta)$.

By using the Assumption 3 we have

$$\mu = z_o \dot{v},$$

and by defining the components of $S^+(\theta)$ as $\pi_{ij}(\theta)$, the i-th friction coefficient can be expressed by

$$\begin{aligned} \mu_i &= z_o \dot{v}_i, \\ \mu_i &= z_o \frac{d}{dt}\left(\pi_{i1}\dot{\tilde{x}}_1 + \ldots + \pi_{i3}\dot{\tilde{\theta}} + \ldots + \pi_{i6}\dot{\tilde{\phi}}_3\right), \\ \mu_i &= z_o \Bigg(\frac{\partial \pi_{i1}}{\partial \tilde{\theta}}\dot{\tilde{\theta}}\dot{\tilde{x}}_1 + \pi_{i1}\ddot{\tilde{x}}_1 \\ &\quad + \frac{\partial \pi_{i2}}{\partial \tilde{\theta}}\dot{\tilde{\theta}}\dot{\tilde{x}}_2 + \pi_{i2}\ddot{\tilde{x}}_2 + \frac{\partial \pi_{i3}}{\partial \tilde{\theta}}\dot{\tilde{\theta}}^2 + \pi_{i3}\ddot{\tilde{\theta}} \\ &\quad + \frac{\partial \pi_{i4}}{\partial \tilde{\theta}}\dot{\tilde{\theta}}\dot{\tilde{\phi}}_1 + \pi_{i4}\ddot{\tilde{\phi}}_1 + \frac{\partial \pi_{i5}}{\partial \tilde{\theta}}\dot{\tilde{\theta}}\dot{\tilde{\phi}}_2 + \pi_{i5}\ddot{\tilde{\phi}}_2 \\ &\quad + \frac{\partial \pi_{i6}}{\partial \tilde{\theta}}\dot{\tilde{\theta}}\dot{\tilde{\phi}}_3 + \pi_{i6}\ddot{\tilde{\phi}}_3\Bigg), \end{aligned}$$

since $S^+(\theta)$ depends only on θ. Taking the time derivative of μ_i yields

$$\begin{aligned} \dot{\mu}_i = z_o \Bigg(& \frac{d}{dt}\left(\frac{\partial \pi_{i1}}{\partial \tilde{\theta}}\dot{\tilde{\theta}}\right)\dot{\tilde{x}}_1 + 4\frac{\partial \pi_{i1}}{\partial \tilde{\theta}}\dot{\tilde{\theta}}\ddot{\tilde{x}}_1 \\ & + \frac{d}{dt}\left(\frac{\partial \pi_{i2}}{\partial \tilde{\theta}}\dot{\tilde{\theta}}\right)\dot{\tilde{x}}_2 + 4\frac{\partial \pi_{i2}}{\partial \tilde{\theta}}\dot{\tilde{\theta}}\ddot{\tilde{x}}_2 \\ & + \frac{d}{dt}\left(\frac{\partial \pi_{i3}}{\partial \tilde{\theta}}\dot{\tilde{\theta}}\right)\dot{\tilde{\theta}} + 5\frac{\partial \pi_{i3}}{\partial \tilde{\theta}}\dot{\tilde{\theta}}\ddot{\tilde{\theta}} \\ & + \frac{d}{dt}\left(\frac{\partial \pi_{i4}}{\partial \tilde{\theta}}\dot{\tilde{\theta}}\right)\dot{\tilde{\phi}}_1 + 4\frac{\partial \pi_{i4}}{\partial \tilde{\theta}}\dot{\tilde{\theta}}\ddot{\tilde{\phi}}_1 \\ & + \frac{d}{dt}\left(\frac{\partial \pi_{i5}}{\partial \tilde{\theta}}\dot{\tilde{\theta}}\right)\dot{\tilde{\phi}}_2 + 4\frac{\partial \pi_{i5}}{\partial \tilde{\theta}}\dot{\tilde{\theta}}\ddot{\tilde{\phi}}_2 \\ & + \frac{d}{dt}\left(\frac{\partial \pi_{i6}}{\partial \tilde{\theta}}\dot{\tilde{\theta}}\right)\dot{\tilde{\phi}}_3 + 4\frac{\partial \pi_{i6}}{\partial \tilde{\theta}}\dot{\tilde{\theta}}\ddot{\tilde{\phi}}_3 \\ & + \pi_{i1}\dddot{\tilde{x}}_1 + \ldots + \pi_{i3}\dddot{\tilde{\theta}} + \ldots + \pi_{i6}\dddot{\tilde{\phi}}_3 \Bigg). \end{aligned} \tag{12}$$

For uniformly accelerated motion, we have that $\dddot{\tilde{x}}_1 \approx 0, \cdots, \dddot{\tilde{\theta}} \approx 0, \cdots, \dddot{\tilde{\phi}}_3 \approx 0$. Thus, one may simplify (12) to

$$\begin{aligned}\dot{\mu} &= z_o \begin{bmatrix} \ddot{\pi}_{i1} & \dots & \ddot{\pi}_{i3} & \dots & \ddot{\pi}_{i6} \end{bmatrix} \dot{\tilde{q}} \\ &\quad + z_o \begin{bmatrix} 4\dot{\pi}_{i1} & \dots & 5\dot{\pi}_{i3} & \dots & 4\dot{\pi}_{i6} \end{bmatrix} \ddot{\tilde{q}} \\ &= z_o \begin{bmatrix} \ddot{\pi}_{i1} & \dots & \ddot{\pi}_{i3} & \dots & \ddot{\pi}_{i6} \end{bmatrix} \dot{\tilde{q}} \\ &\quad + z_o \begin{bmatrix} \dot{\pi}_{i1} & \dots & \dot{\pi}_{i3} & \dots & \dot{\pi}_{i6} \end{bmatrix} \Gamma \ddot{\tilde{q}} \end{aligned} \quad (13)$$

where $\Gamma \triangleq \text{diag}\,(4\ 4\ 5\ 4\ 4\ 4)$.

By using (10) and the chain rule for differentiation,

$$\frac{ds_i}{dt} = \frac{ds_i}{d\mu_i}\dot{\mu}_i = \left(\frac{1}{c_2 e^{-c_2\mu_i} - c_3}\right)\dot{\mu}_i,$$

one may use (13) to obtain

$$\begin{aligned}\dot{s}_i = z_o \left(\frac{1}{c_2 e^{-c_2\mu_i} - c_3}\right) &\left([\ddot{\pi}_{i1} \ \dots \ \ddot{\pi}_{i3} \ \dots \ \ddot{\pi}_{i6}]\, \dot{\tilde{q}}\right. \\ &\left. + [\dot{\pi}_{i1} \ \dots \ \dot{\pi}_{i3} \ \dots \ \dot{\pi}_{i6}]\, \Gamma\, \ddot{\tilde{q}}\right), \end{aligned} \quad (14)$$

as an alternative expression for $\dot{s}_i$. However, since $s \neq 0$ and the map in (10) is a $\mathcal{C}^1$-diffeomorphism then

$$z_o \underbrace{\left(\frac{1}{c_2 e^{-c_2\mu_i} - c_3}\right)}_{\frac{ds_i}{d\mu_i}} \neq 0, \forall t. \quad (15)$$

Now, defining that

$$R_\mu \triangleq \text{diag}\begin{pmatrix} z_o\frac{ds_1}{d\mu_1} & z_o\frac{ds_2}{d\mu_2} & z_o\frac{ds_3}{d\mu_3} \end{pmatrix}, \ \forall\, s,$$

one may express (14) in the following compact form

$$\dot{s} = R_\mu \ddot{S}^+(\theta)\dot{\tilde{q}} + R_\mu \dot{S}^+(\theta)\Gamma\ddot{\tilde{q}}. \quad (16)$$

3.2 Measuring the traction performance

The above expression gives an alternative differential equation to represent the rolling dynamic at the wheels and with it, we can analyze if the appropriate rolling conditions in (11) are satisfied. Thus, by using of the 2-norm $\|\cdot\|_2$, our objetive can be defined by

$$\|\dot{s}\|_2 \to 0, \ \text{ when } t \to \infty. \quad (17)$$

4 Control on an invariant manifold

An invariant manifold for slip is introduced and defined by

$$s = H_\varepsilon(x, u_\varepsilon, \varepsilon) \quad (18)$$

in order to make that the tracking error will converge to zero and it guaranteing the appropriate rolling conditions for a smooth feedback control law u_ε.

4.1 Computing the invariant manifold

We prefer to construct the linearizing control law as well as the corresponding H_ε assuming these functions to be analytic. Thus, these functions and their time derivatives can be developed under the form of Taylor series expansion:

$$u_\varepsilon = u_0 + \varepsilon u_1 + \varepsilon^2 u_2 + \ldots + \varepsilon^N u_N \quad (19)$$

$$H_\varepsilon = H_0 + \varepsilon H_1 + \varepsilon^2 H_2 + \ldots + \varepsilon^N H_N \quad (20)$$

$$\dot{H}_\varepsilon = \dot{H}_0 + \varepsilon \dot{H}_1 + \varepsilon^2 \dot{H}_2 + \ldots + \varepsilon^N \dot{H}_N, \quad (21)$$

where N can be considered a robust term.

By substituting (19)-(21) in (5)-(6) gives

$$\begin{aligned}\dot{x} = B_0(q)v + B_2(q)H_0 + B_3(q)u_0 + \\ \varepsilon\left[B_1(q)H_0 + B_2(q)H_1 + B_3(q)u_1\right] + \\ \varepsilon^2\left[B_1(q)H_1 + B_2(q)H_2 + B_3(q)u_2\right] + \ldots \\ \varepsilon^N\left[B_1(q)H_{N-1} + B_2(q)H_N + B_3(q)u_N\right] \end{aligned} \quad (22)$$

and

$$\begin{aligned}\varepsilon\left[\dot{H}_0 + \varepsilon\dot{H}_1 + \varepsilon^2\dot{H}_2 + \ldots + \varepsilon^N\dot{H}_N\right] = \\ C_0(q)\,v + C_2(q)\,H_0 + C_3(q)\,u_0 + \\ \varepsilon\left[C_1(q)H_0 + C_2(q)H_1 + C_3(q)u_1\right] + \\ \varepsilon^2\left[C_1(q)H_1 + C_2(q)H_2 + C_3(q)u_2\right] + \ldots \\ \varepsilon^N\left[C_1(q)H_{N-1} + C_2(q)H_N + C_3(q)u_N\right], \end{aligned} \quad (23)$$

and equating like powers of ε in (23) gives the following recursive expression for the terms H_k, for $i = 1, \ldots, N$, in (20):

$$H_k = C_2^{-1}(q)\left[\dot{H}_{k-1} - C_1(q)H_{k-1} - C_3(q)u_k\right]. \quad (24)$$

For $k = 0$, (24) do not offer sufficient information to calculate H_0 in (20). So, from (6), for $\varepsilon = 0$, the component H_0 can be calculated as

$$H_0 = -\,C_2^{-1}(q)\left[C_0(q)\,v + C_3(q)\,u_0\right], \quad (25)$$

where u_0 is the first component into the Taylor serie expansion defined in (19). The eq. (25) is knowing as "slow" manifold. The terms H_k for $k > 0$ implies that the trajectories of system (5)-(7) move on a slight variation of the "slow" manifold[1]. In the same way, u_k for $k > 0$ implies that the control law is composed by the main control law, in this work defined by u_0, and the corrective control actions [i.e., the terms with powers of ε greater than 0 in (19)].

4.2 Control design

The control law is projected on the inverse dynamics of (4) and the output equation (8). This is defined by

$$u_0 = \left[S^T(\theta)B\right]^{-1}\left[S^T(\theta)MS(\theta)\right]E^{-1}(\theta)\left[\rho - \dot{E}(\theta)\,v\right] \quad (26)$$

with

$$E(\theta) = \frac{\partial P_0(\theta)}{\partial(x_1, x_2, \theta)}\,S_1(\theta) = \begin{bmatrix} \cos\theta & \sin\theta & -L\cos\theta \\ -\sin\theta & \cos\theta & -L\sin\theta \end{bmatrix}$$

ensures the dynamics of AxeBot to be $\dot{v} = \rho$, where ρ is an auxiliar control variable defined by

$$\rho = \left[\ddot{x}_1^r \ \ddot{x}_2^r \ \ddot{\theta}^r\right]^T - K_2\,e - K_1\,\dot{e} \quad (27)$$

in order to insure tracking of the reference trajectory defined by the vector $[x_1^r \ x_2^r \ \theta^r]^T$. The tracking error, e, and its derivative, $\dot{e}$, are defined by

$$\begin{aligned} e &= [x_1 \ x_2 \ \theta]^T - [x_1^r \ x_2^r \ \theta^r]^T \\ \dot{e} &= S_1(\theta)v + A_1(\theta)\varepsilon H_\varepsilon - \left[\dot{x}_1^r \ \dot{x}_2^r \ \dot{\theta}^r\right]^T \end{aligned}$$

where H_ε is the manifold defined in (18) and $\{K_1\,,\,K_2\} \subseteq \mathbb{R}^{3\times 3}$ are arbitrary positive definite matrices such that the desired dynamic represented by (27) is Hurwitz (Motte and Campion, 2000).

[1] That slight variation of the "slow" manifold is called the "fast" manifold.

4.3 Computing the corrective control actions

From (22), the set of corrective controls $u_1, u_2, \ldots, u_N$ are simply designed to annihilate the set of terms $\varepsilon, \varepsilon^2, \ldots, \varepsilon^N$, respectively. That is,

$$\begin{aligned} u_1 &= -B_3^+(q)\,[B_1(q)H_0 + B_2(q)H_1] \\ u_2 &= -B_3^+(q)\,[B_1(q)H_1 + B_2(q)H_2] \\ &\vdots \\ u_k &= -B_3^+(q)\,[B_1(q)H_{k-1} + B_2(q)H_k] \end{aligned} \tag{28}$$

for $k = 1, 2, \ldots, N$, where $B_3^+(q)$ is the pseudo-inverse of $B_3(q)$.

5 Experimental results

The manifold defined by (18) and the rolling dynamic defined by (16) allow to evaluate of the control laws used for the trajectory tracking in the omnidirectional robot AxeBot and to observe how the corrective control actions attenuate the violation at the appropriate rolling conditions.

In this work we projected two corrective controls, i.e., the degree of robustness is $N = 2$ and the corrective control actions u_1, u_2 are associated to the annihilation of ε and ε^2. Thus, by using (28) these corrective controls are:

$$u_1 = (B_2C_2^{-1}C_3 - B_3)^+ \Big(B_1H_0 + B_2C_2^{-1}\dot{H}_0 - B_2C_2^{-1}C_1H_0\Big)$$

and

$$\begin{aligned} u_2 = (B_3 - B_2C_2^{-1}C_3)^+ \Big[& (B_2C_2^{-1}C_2^{-1}C_3)\dot{u}_1 \\ & - (B_2C_2^{-1}C_1C_2^{-1}C_3 - B_1C_2^{-1}C_3)u_1 \\ & - B_2C_2^{-1}C_2^{-1}\ddot{H}_0 - \Big(B_2C_2^{-1}C_1C_2^{-1}C_1 \\ & - B_1C_2^{-1}C_1\Big)H_0 - (B_1C_2^{-1} \\ & - B_2C_2^{-1}C_2^{-1}C_1 - B_2C_2^{-1}C_1C_2^{-1}\Big)\dot{H}_0\Big]. \end{aligned}$$

The experimental platform AxeBot is composed of two main modules: a microprocessor system responsible for the implementation of the instrumentation and the time base generation module (sample time of 50 ms) that creates a real time clock. The high-level controllers are implemented on a personal computer. These modules communicate through a Zigbee platform composed by two Maxstream's Xbee modules. The robot odometry data and the control signals (motors voltages) are transmitted serially through 32-byte packets at a rate of 57600 b/s. The DC motors are of A-max 22 type (nominal voltage: 6 V, power rating: 5 W) developed by Maxon Motors, and they are controlled by H-bridge circuits made by Acroname Robotics (part no. S17-3A-LV-BRIDGE). The control algorithms were implemented via Lazarus IDE software for Linux/Ubuntu operation systems on a Pentium Core i7 @ 2.8 GHz.

The parameters used in the experiments are: $L = 0.12\,\text{m}$, $r = 0.0349\,\text{m}$, $M = 1.83\,\text{Kg}$, $I_c = 0.0132$ Kg-m^2, $I_w = 0.216 \times 10^{-4}$ Kg-m^2, $\delta = 0.1$. To analyzing the rolling performance the matrix R_μ is defined as:

$$\begin{aligned} R_\mu &= \text{diag}\left(z_o \tfrac{ds_1}{d\mu_1}\Big|_{s\sim 0}\; z_o \tfrac{ds_2}{d\mu_2}\Big|_{s\sim 0}\; z_o \tfrac{ds_3}{d\mu_3}\Big|_{s\sim 0} \right) \\ &= \text{diag}\left(z_o\eta \;\; z_o\eta \;\; z_o\eta \right) \end{aligned}$$

with $z_o = 5.620 \times 10^{-3}$ (with $M_r = 0.0336$ Kg) and by considering small values of longitudinal slip (less than 0.1) the derivatives $\frac{ds_i}{d\mu_i}$ are approximated by $\eta = 10/19$. From Assumption 1, $\varepsilon = 10^{-10}$ for $D = 4\times10^9$ and $G = 10^{10}$. The reference dynamic was defined by $K_1 = 23\, I_{3\times3}$ and $K_2 = 70\, I_{3\times3}$ which is a critically damped second-order system with poles at -19.38 and -3.61. The reference trajectory is a circle with radius 1 m.

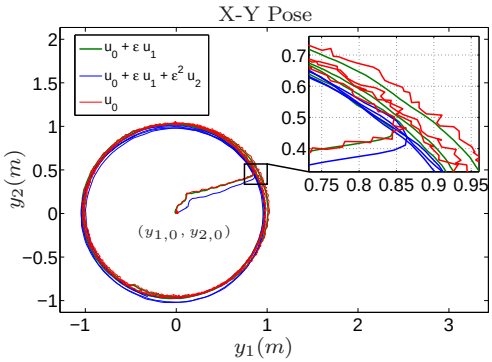

Figura 2: Trajectory tracking for a circle reference. Initial pose: $x_{1,0} = 0m, x_{2,0} = -0.12m, \theta_0 = 0$ rad ($y_{1,0} = 0m, y_{2,0} = 0m$).

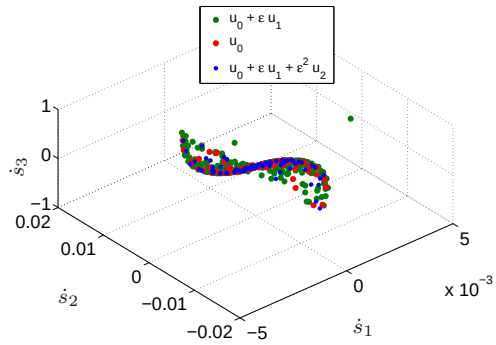

Figura 3: Behavior of $\dot{s}$ around the rolling condition $\dot{s} = (0, 0, 0)$.

In this paper was used (16) and (17) as a way to observing the rolling performance of mobile base at different reference trajectories at experimental results and finally to choose the suitable control law.

5.1 Circular trajectory and discussion of results

In Fig. 2 is shown the trajectory tracking of the circle. In Fig. 3 is shown the behavior of $\dot{s}$ around the condition $\dot{s} = (0, 0, 0)$. Clearly, the concentration of all points associated with this slip rate $\dot{s}$ are around the origin (0,0,0). In the time domain the norm $\|\dot{s}\|_2$ was used as a way of understanding the total behavior of slip into the overall dynamic of Axebot (see Fig. 4). The behavior observed at Fig. 4 show that the appropriate rolling condition $\dot{s} = 0$ defined by (11) has a behavior more near to zero when used the control law with two corrective control actions [i.e., $u_0+\varepsilon u_1+\varepsilon^2 u_2$] (see the inset at Fig. 4). The other condition $s \neq 0$ is a direct consequence of the behavior of norm $\|\dot{s}\|$ when $t \to \infty$. To explain this, one can proof that the kinematic constraints are not ever satisfied, i.e. $A^T(q)\dot{q} \neq 0$.

From observations in Fig. 4 we can affirm that $\|\dot{s}\| \to 0$ for $t \to \infty$. Consequently, $\lim_{t\to\infty} \dot{s} = 0$

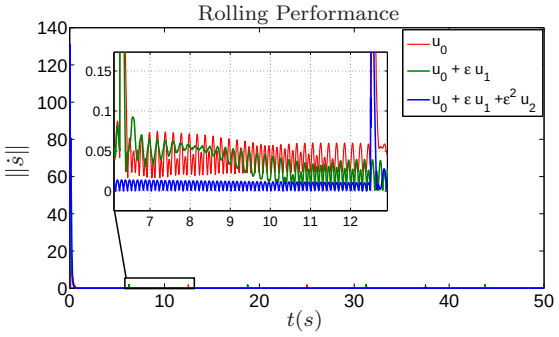

Figura 4: Evolution of the norm $\|\dot{s}\|$ on time domain. For small values of longitudinal slip (less than 0.1) the derivatives $\frac{ds_i}{d\mu_i}$ into the term R_μ were approximated by $\eta = 10/19$.

and $\lim_{t\to\infty} s > 0$, or $\lim_{t\to\infty} s < 0$, or $\lim_{t\to\infty} s = 0$. Multiplying both sides of (2) by $A^T(\theta)$ yields

$$\begin{aligned} A^T(\theta)\dot{q} &= A^T(\theta)S(\theta)v + A^T(\theta)A(\theta)\varepsilon s \\ &= A^T(\theta)A(\theta)\varepsilon s \qquad \text{(By using (3))} \end{aligned} \quad (29)$$

and since the model (5)-(7) assume that the kinematic constraints are not satisfied [i.e., $A^T(q)\dot{q} \neq 0$ and $\varepsilon \neq 0$], then can be verified that the option $\lim_{t\to\infty} s = 0$ contradize this assumption when such option is substituted in (29). Thus

$$\lim_{t\to\infty} s \neq 0$$

and we have proved the satisfaction of the appropriate rolling condition $s \neq 0$.

6 Final remarks

Here, we used an alternative expression for the rolling in an omnidirectional robot [the AxeBot] to observing the slip behavior around the appropriate rolling conditions, $\dot{s} = 0$ and $s \neq 0$. Considering the slip as a fast variable within the overall dynamic of the mobile robot is proposed a model based on theory of singular perturbations and consequently projected corrective control actions that mitigate the influence of the slip. The AxeBot has a mechanism of self-localization in the workspace based on odometry, thus the AxeBot give us a convenient problem-situation to testing problems arising from the presence of slip at the wheels. With the experimental information associated with the trajectory tracking is used the norm of the slip rate defined by (16) as support to choosing what is the suitable control law.

Currently, the methodology presented in this paper will be extended for wheeled mobile robots with nonholonomic and quasi-holonomic kinematic constraints that have controllers based in others theoretical approaches different of the singular perturbation theory.

Agradecimentos

The authors would like to thank *Conselho Nacional de Desenvolvimento Científico e Tecnológico* (CNPq), *Coordenação de Aperfeiçoamento de Pessoal de Nível Superior* (CAPES), and *Fundação de Amparo à Pesquisa do Estado da Bahia* (FAPESB), all of them of Brazil, for the research grant, financial support and study fellowship.

Referências

Bahari, N., Becker, M. and Firouzi, H. (2008). Feature based localization in an indoor environment for a mobile robot based on odometry, laser, and panoramic vision data, *ABCM Symposium Series in Mechatronics*, Vol. 3, Rio de Janeiro, Brazil, pp. 266 – 275.

Balakrishna, R. and Ghosal, A. (1995). Modeling of slip for wheeled mobile robots, *IEEE Transactions on Robotics and Automation* **11**(1): 126–132.

Canudas de Wit, C., Tsiotras, P., Velenis, E., Basset, M. and Gissinger, G. (2003). Dynamic friction models for road/tire longitudinal interaction, *Vehicle System Dynamics* **39**(3): 189–226.

D'andréa-novel, B., Campion, G. and Bastin, G. (1995). Control of wheeled mobile robots not satisfying ideal velocity constraints: A singular perturbation approach, *International Journal of Robust and Nonlinear Control* **5**(4): 243–267.

Fernández, C. A. P. and Cerqueira, J. J. F. (2009a). Control de velocidad con compensación de deslizamiento en las ruedas de una base holonómica usando un neurocontrolador basado en el modelo narma-l2, *IX Congresso Brasileiro de Redes Neurais*, Ouro Preto - Brasil.

Fernández, C. A. P. and Cerqueira, J. J. F. (2009b). Identificação de uma base holonômica para robôs moveis com escorregamento nas rodas usando um modelo narmax polinomial, *IX Simpósio Brasileiro de Automação Inteligente*, Brasilia D.F - Brasil.

Fernández, C. A. P., Cerqueira, J. J. F. and Lima, A. M. N. (2012). Dinâmica não-linear do escorregamento de um robô móvel omnidirecional com restrição de rolamento, *XIX Congresso Brasileiro de Automática*, Campina Grande - Brasil.

Ivankjo, E., Petrović, I. and Vašak, M. (2004). Sonar-based pose tracking of indoor mobile robots, *Journal for Control, Measurement, Electronics, Computing and Communications* **45**(3-4): 145–154.

Motte, I. and Campion, G. (2000). A slow manifold approach for the control of mobile robots not satisfying the kinematic constraints, *IEEE Transactions on Robotics and Automation* **16**(6): 875 –880.

Song, K.-T. and Wang, C.-W. (2009). Self-localization and control of an omni-directional mobile robot based on an omni-directional camera, *Conf. Rec. IEEE/ASCC*, Hong Kong, China, pp. 899 –904.

Trojnacki, M. (2013). Modeling and motion simulation of a three-wheeled mobile robot with front wheel driven and steered taking into account wheels slip, *Archive of Applied Mechanics* **83**(1): 109–124.